


Two-mode squeezing in Floquet-engineered power-law interacting spin modelsArman Duha  and Thomas Bilitewski *Department of Physics, Oklahoma State University, Stillwater, Oklahoma 74078, USA* (Received 11 March 2024; accepted 12 June 2024; published 26 June 2024)

We study the nonequilibrium dynamics of a quantum spin-1/2 XXZ model confined in a two-dimensional bilayer system, with couplings mediated by inverse power-law interactions, falling off with distance r as $1/r^\alpha$, with spatiotemporal control of the spins enabled via local fields. An initial state of spins with opposite magnetization in the two layers is dynamically unstable resulting in exponential generation of correlated pairs of excitations. We find that scalable generation of entanglement in the form of two-mode squeezing between the layers can generically be achieved in power-law models. We further demonstrate that spatially temporally engineered interactions allow one to significantly increase the generated entanglement and in fact achieve Heisenberg limited scaling. This work is relevant to a wide variety of experimental atomic, molecular, and optical platforms, which realize power-law spin models, and demonstrates the advantage of spatiotemporal control to maximize the generation of metrologically useful entanglement, with potential applications in quantum-enhanced sensing.

DOI: [10.1103/PhysRevA.109.L061304](https://doi.org/10.1103/PhysRevA.109.L061304)

Introduction. Long-range interacting spin models realized in quantum gases of polar molecules [1–3], magnetic atoms [4], Rydberg atoms [5,6], or trapped ions [7] are emerging as promising platforms for quantum simulation [7–10], computation [11–13], and quantum metrology [14]. These systems with the advent of quantum gas microscopes and tweezers [15–20] now combine the presence of long-range interactions with the capability to control, manipulate, and measure at the single-particle level in a site-resolved fashion. In addition to spatial control and resolution the ability to design the interactions is required to realize fully programable quantum simulators. A particularly powerful approach to the engineering of spin interactions is time-periodic driving or Floquet engineering [21,22] and control of the interactions via pulse sequences [23,24]. Indeed, this temporal control enables the desired programability of the interactions as demonstrated in cavities [25], Rydberg atoms [26–28], polar molecules [18,29], and trapped ions [30].

One particular direction in the quest for quantum advantage enabled by these advances is the enhancement of sensitivity of measurements via entanglement in the form of spin squeezing [31,32]. While spin squeezing had been achieved for infinite-range interactions and via quantum non-demolition (QND) measurements [33–38], only recently have experiments demonstrated this for finite-range interactions in trapped ions and Rydberg arrays [39–42]. The majority of these works has thus far focused on homogeneous globally collective initial states interacting via homogeneous interactions and global controls, not exploiting the advantage offered by fully controllable quantum platforms.

We go beyond this paradigm and demonstrate how spatiotemporal control, i.e., spatially dependent temporal control, applied to spatially patterned, structured initial states confer additional tangible benefits for entanglement generation. Specifically, we demonstrate how to achieve Heisenberg limited scaling of two-mode squeezing via Floquet-engineered spatially anisotropic interactions in bilayers of power-law

interacting XXZ spin models. Two-mode squeezing (TMS) [43–45] is a process generating entanglement via the production of pairs of particles, a process underlying phenomena from the fundamental in the Einstein-Podolsky-Rosen (EPR) paradox [46], over Unruh thermal radiation [47] and the Schwinger effect [48,49] to the applied in parametric amplification in quantum optics [43]. Two-mode squeezing is well established in photonic systems [43,50] and has been realized in thermal gases [51,52], and in Bose-Einstein condensates of ultracold atoms interacting via contact interactions [53–59], where it has been successfully used for EPR steering [60–62]. More recently it has been proposed as a mechanism to generate metrologically useful entanglement between spin ensembles in cavities via light-mediated interactions [63] and in dipolar systems [64,65]. There long-range interactions naturally create entanglement in spatially separated ensembles, with the additional benefit of single-site single-particle control over these entangled states.

Here, we investigate the two-mode squeezing dynamics of spin-1/2 bilayers with power-law interactions, scaling as $r^{-\alpha}$ with the distance r . We find that finite-range interactions ($\alpha = 1, 2, 3$) achieve the same amount of squeezing as infinite-range ($\alpha = 0$) interactions for sufficiently widely separated layers. By Floquet engineering spatially anisotropic interactions adapted to the initial state and desired entanglement dynamics we improve the $1/\sqrt{N}$ scaling of the sensitivity in system size N to the ultimate Heisenberg limit of $1/N$.

Our work thus opens up new opportunities to exponentially generate metrologically useful entanglement in a variety of platforms including Rydberg atoms ($\alpha = 3, 6$) [5,6], polar molecules ($\alpha = 3$) [1–3], magnetic atoms ($\alpha = 3$) [4], and trapped ions ($1 < \alpha < 3$) [7], wherein single site [18], layer selective control [66], and Floquet engineering [23,26,29] have been demonstrated and which can realize bilayer structures [29,66–68].

Model. We consider a two-dimensional bilayer of spins interacting via long-range interactions as shown in Fig. 1(a).

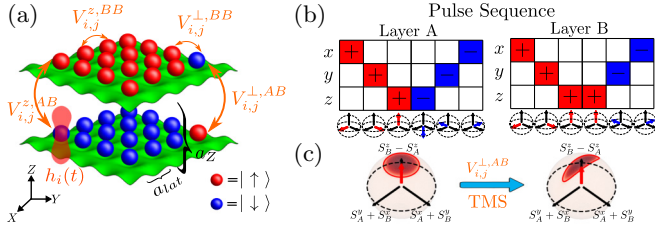


FIG. 1. (a) Illustration of spin-1/2 model confined in a bilayer interacting via power-law interactions with Ising V^z and spin-exchange V^\perp and intralayer (AA, BB) and interlayer (AB) terms. Spins can be locally addressed via fields $h_i(t)$. (b) Layer pulse sequence in toggling frame (see text) to symmetrize intralayer Ising and cancel interlayer Ising interactions. (c) Bloch sphere of mixed quadratures that are squeezed by the interplane spin-exchange interactions.

The two layers, denoted as A and B , both have a square geometry with lattice spacing a_{lat} and are separated by a tunable distance a_z . The spins have two internal states and the dynamics is governed by a spin-1/2 XXZ Hamiltonian

$$\hat{H} = 1/2 \sum_{i \neq j} V_{ij} \left[\frac{V_\perp}{2} (\hat{s}_i^+ \hat{s}_j^- + \hat{s}_i^- \hat{s}_j^+) + V_z \hat{s}_i^z \hat{s}_j^z \right] + \sum_i h_{i,x}(t) \hat{s}_i^x + h_{i,y}(t) \hat{s}_i^y + h_{i,z}(t) \hat{s}_i^z, \quad (1)$$

where \mathbf{i}, \mathbf{j} are three-dimensional indices (i_x, i_y, i_z), specifying the layer-index i_z and positions i_x, i_y in the layer of size $L \times L$ with $N = L^2$ spins in each layer. The spin operators $\hat{s}_i^\mu = \hat{\sigma}_i^\mu / 2$, with the Pauli matrices $\hat{\sigma}^\mu$, act on the spin at site \mathbf{i} . We consider power-law interactions of the form $V_{ij} = |\mathbf{r}_i - \mathbf{r}_j|^{-\alpha}$ and V_\perp and V_z describe the relative strengths of the spin-exchange and Ising interactions. While these interactions only depend on distance to appeal to a range of systems, spatial anisotropy, as natural for dipolar ($\alpha = 3$) interactions and studied before [65], is not expected to change the results of this work. We include time and position dependent fields to control the spins in the second line of Eq. (1).

Engineering optimal two-mode squeezing. Starting from oppositely polarized layers, $\vec{S}_\eta = \sum_{i \in \eta} \vec{s}_i = \pm N/2 \hat{z}$, the goal is to utilize spin-spin interactions to generate entangled pairs of collective excitations between the layers.

The initial state is an eigenstate of intralayer Heisenberg ($\vec{s}_i \cdot \vec{s}_j$) interactions, which will protect the collective layer spin by energetically penalizing noncollective excitations. In contrast, the interlayer spin-exchange interactions will create pairs of flipped spins and the interlayer Ising interactions will energetically penalize the creation of spin flips [64,65], eventually arresting pair production. Thus Heisenberg intralayer interactions are required to realize collective dynamics (for finite-range interactions), whereas Ising interactions between layers are detrimental. This suggests two strategies: (i) utilizing Heisenberg interactions and canceling the interlayer Ising interactions to leading order by a static field or (ii) fully removing only the Ising interlayer interactions, while keeping Heisenberg intralayer interactions.

The first strategy corresponds to fully symmetric Heisenberg interactions ($V_z = V_\perp$) and a staggered layer-dependent z

field, i.e.,

$$\hat{H}_h = 1/2 \sum_{ij} V_{ij} \vec{s}_i \cdot \vec{s}_j + h (\hat{S}_B^z - \hat{S}_A^z), \quad (2)$$

where the local z field exactly cancels the energy cost due to the interlayer Ising interactions of creating one collective spin flip in each layer on top of the initial state, $h = 1/(2N) \sum_{i \in A, j \in B} V_{ij} = NV_{\text{avg}}/2$.

The second strategy corresponds to engineering

$$\hat{H}_V = 1/2 \sum_{\eta} \sum_{i,j \in \eta} V_{ij} \vec{s}_i \cdot \vec{s}_j + \sum_{i \in A, j \in B} V_{ij} (\hat{s}_i^x \hat{s}_j^x + \hat{s}_i^y \hat{s}_j^y), \quad (3)$$

where the first term describes intralayer Heisenberg and the second term interlayer spin-exchange interactions.

We achieve this by extending interaction design via global pulses [23] to layer-dependent pulse sequences utilizing local control of the spins. Starting from Ising interactions, $\hat{s}_i^z \hat{s}_j^z$, applying a rotation from z to direction $\alpha(\beta)$ to the first (second) spin transforms the interactions to $\hat{s}_i^\alpha \hat{s}_j^\beta$. The resulting interactions under a sequence of rotations can therefore be represented by the orientation of the z operator during the k th step of the sequence, i.e., in the toggling-frame representation [23]. Using the six step layer-dependent sequence illustrated in Fig. 1(b), Ising interactions are successively transformed into xx, yy , and zz interactions in steps 1 to 3, both within and between the layers. Crucially, in step 4 by applying different pulses to layers A and B we obtain positive intralayer zz , but negative interlayer zz interactions, followed by yy and xx interactions in steps 5 and 6. Thus this sequence fully symmetrizes the intraplane Ising to Heisenberg interactions and only generates $xx + yy$ interlayer interactions from the original interlayer Ising interactions. The average Hamiltonian then is Eq. (3) with an overall prefactor of $V_z/3$, which is absorbed in V_{avg} .

In the following we will work directly with the target Hamiltonian, rather than the explicit pulse sequence. We have checked convergence of the dynamics under this multistep Floquet protocol to the desired dynamics as a function of the Floquet period [69], which shows good agreement if the total sequence takes about half of a nearest-neighbor interaction time, $T \approx 0.6V_{\text{NN}}/\hbar$, which is well within reach of experimental platforms [23,29].

For both scenarios the fully collective regime can be understood in terms of Holstein-Primakoff bosons [70] of the collective layer spins, which in first order are $S_A^z = -N/2 + \hat{a}^\dagger \hat{a}$, $S_A^+ = \hat{a}$, $S_A^- = \hat{a}^\dagger$, $S_B^z = N/2 - \hat{b}^\dagger \hat{b}$, $S_B^- = \hat{b}$, and $S_B^+ = \hat{b}^\dagger$. In terms of these we obtain $H_{\text{TMS}} = NV_{\text{avg}}(\hat{a}^\dagger \hat{b}^\dagger + \hat{a} \hat{b})/2$, which is the desired two-mode squeezing Hamiltonian [43–45]. The number of generated entangled excitations $n_{\text{ex}} = \hat{a}^\dagger \hat{a} + \hat{b}^\dagger \hat{b} = S_A^z - S_B^z + N$ within TMS is predicted to grow exponentially $n_{\text{ex}} = 2 \sinh^2[NV_{\text{avg}}t/(2\hbar)]$ [43–45]. The generated entanglement results in squeezing of mixed quadratures between the collective layer spins. The squeezed quadratures correspond to $S_A^z + S_B^z$ and $S_A^y - S_B^y$, while the antisqueezed quadratures correspond to $S_A^z - S_B^z$ and $S_A^y + S_B^y$. These show exponentially decreasing or growing variances $\text{Var}[\mathcal{O}^\pm] = N/2 e^{\pm NV_{\text{avg}}t/\hbar}$. We illustrate these quadratures on the Bloch sphere for the initial state, as well as the squeezed state in Fig. 1(c).

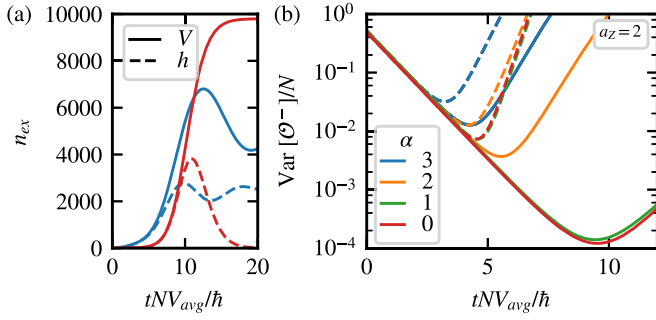


FIG. 2. Pair creation and two-mode squeezing via Floquet-engineered spatially anisotropic interactions. (a) Number of created excitations $n_{\text{ex}} = S_A^z - S_B^z + N$. (b) Time evolution of variance of the squeezed quadrature. In both panels for the Floquet-engineered model (solid lines, V) and for the staggered field model (dashed, h) for a range of interaction power-law exponents α at fixed layer distance $a_z = 2$.

The main difference between these two approaches is that in the staggered field case the interlayer Ising interactions were canceled by the h field up to quadratic order, whereas in the Floquet-engineered case the Ising interactions were removed at the Hamiltonian level. Thus, in quadratic order, both approaches are equivalent; however, we will show that the second approach provides dramatic improvements over the first.

To substantiate the arguments based on the mapping to bosons in the collective limit we simulate the quantum many-body nonequilibrium dynamics of the spin model using the discrete truncated Wigner approximation (dTWA) [71,72] for up to $2N = 2 \times 70^2 = 9800$ spins. This semiclassical phase space method is expected to be good in the collective regime and has been shown to be accurate even for nearest-neighbor interactions in two-dimensional systems [73]. We provide benchmarks for the current model in the Supplemental Material [69].

Pair creation and squeezing. In Fig. 2(a) we show the generated excitations for infinite-range ($\alpha = 0$) and finite-range ($\alpha = 3$) interactions for the staggered z field (dashed) and the Floquet-engineered model (solid). The Floquet model for infinite-range interactions creates the maximal number of possible excitations, $n_{\text{ex}} = 2N$, fully flipping the layer spin, in contrast to the staggered field case which saturates at a lower number due to the detuning of the pair creation process at finite number of excitations. The same advantage is observed for finite-range interactions, with the Floquet model reaching a significantly higher number of generated pairs. The fully collective model ($\alpha = 0$) here follows the TMS prediction (not shown), until corrections due to the finite spin length become relevant. In contrast, the dipolar case ($\alpha = 3$) at this layer separation $a_z = 2$ quickly deviates, which we understand to be due to noncollective spin dynamics as we will confirm below [69]. We next investigate the squeezing behavior under the same circumstances. In Fig. 2(b) we demonstrate the exponential decrease of the variance of the squeezed quadratures, $\text{Var}[S_A^x + S_B^y] = \text{Var}[S_A^y - S_B^x] \equiv \text{Var}[\mathcal{O}^-]$, for different interaction ranges. We see that the spin dynamics follows the two-mode squeezing prediction

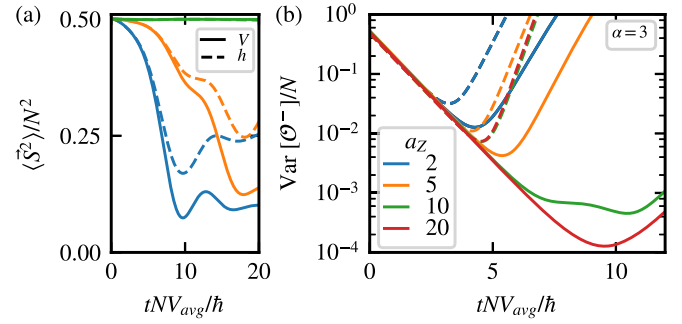


FIG. 3. Collective two-mode squeezing with finite-range interactions. (a) Length of collective layer spins $\langle \tilde{S}_A^2 + \tilde{S}_B^2 \rangle$ with $\hat{S}_{A(B)}^\mu = \sum_{i \in A(B)} \hat{S}_i^\mu$. (b) Time evolution of variance of the squeezed quadrature. In both panels for the Floquet-engineered model (solid lines, V) and for the staggered field model (dashed, h) for a range of layer spacings a_z with fixed power-law exponent $\alpha = 3$.

$\text{Var}[\mathcal{O}^-] = N/2 e^{-NV_{\text{avg}}t/\hbar}$ up until a saturation point of minimal variance. Interestingly, the noncollective spin dynamics of the finite-range model observed in the increased pair number does not seem to affect the variance, suggesting that noncollective spin excitations, affecting the spin polarization, but not the variance, occur on top of the collective squeezing dynamics. While all models show identical short-time evolution, the saturation point depends on the model and interaction exponent α . The Floquet model achieves a significantly lower variance and thus a larger amount of squeezing and sensitivity for all interaction ranges. This is most notable for the infinite-range case, where we observe a two orders of magnitude improvement, but holds true for all interaction ranges α . The reduced improvement for finite-range interactions is again explained by noncollective dynamics as we show next.

Achieving the infinite-range limit. Despite the significant improvement of the achievable squeezing using the Floquet protocol, we observe that the finite-range interaction cases do not saturate to the infinite-range model. This is due to the strong spatial inhomogeneity of the interlayer interaction at short interlayer separations $a_z = 2$ and the resulting noncollective excitations. We therefore explore the tunability of the layer spacing a_z to overcome this limitation in Fig. 3 in the case of dipolar interactions. We first study the collectiveness of the dynamics in terms of the length of the layer spins, $\langle \tilde{S}_A^2 + \tilde{S}_B^2 \rangle$, in Fig. 3(a), demonstrating that as the layer spacing increases the dynamics changes from a regime in which the collective layer spin rapidly dephases at short layer distances to fully collective behavior at larger spacings, where the layer spins stay fully collective with $\tilde{S}_i^2 = N^2/4$. We note that as expected longer-ranged interactions (smaller α) achieve the collective regime for shorter layer distances; we provide data for $\alpha = 1, 2, 3$ in the Supplemental Material [69]. As a direct consequence in Fig. 3(b), which shows the time evolution of the variance of the squeezed quadrature, we observe that the achievable squeezing increases with layer distance. We note that the variance is actually more sensitive than the spin length, showing increases of the minimal squeezing in a regime where the spin length appears fully collective already. Most importantly, the achievable squeezing in the dipolar

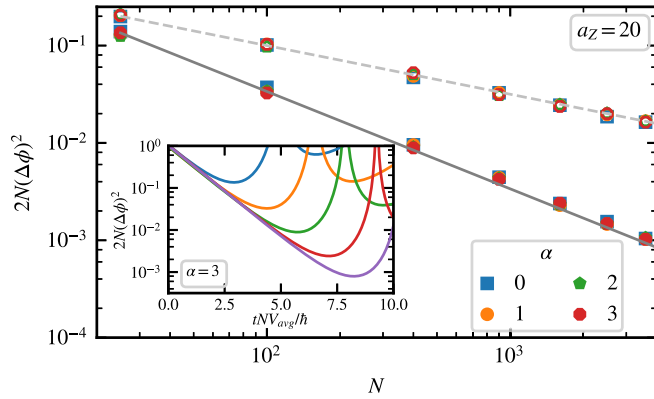


FIG. 4. Heisenberg scaling of sensitivity. Main panel: system size scaling of scaled sensitivity. Different symbols indicate exponent of interactions α , filled symbols for Floquet-engineered model (V), and open symbols for staggered field (h). Solid lines are a guide to the eye for $1/\sqrt{N}$ scaling (light gray) and Heisenberg $1/N$ scaling (dark gray). Inset: time dependence of scaled sensitivity for different system sizes $L = 5, 10, 20, 40, 70$ (top to bottom) at fixed α and a_z for the Floquet model.

($\alpha = 3$) saturates to the infinite-range model [cf. Figs. 2(b) and 3(b)] at sufficiently large layer spacings. Thus finite-range interactions are able to achieve the same amount of squeezing as infinite-range, fully collective interactions.

Heisenberg scaling of sensitivity. The squeezed variance of the generated entangled state directly results in an improved sensitivity of measuring a phase of rotation ϕ around $\hat{S}_A^z - \hat{S}_B^z$ in Ramsey protocols [63] as

$$(\Delta\phi)^2 = \frac{(\Delta\mathcal{O})^2}{(\hat{S}_A^z - \hat{S}_B^z)^2} \quad (4)$$

and a corresponding enhancement over using $2N$ unentangled particles $2N(\Delta\phi)^2$. As the state gets squeezed the variance decreases exponentially; however, at the same time the polarized spin component is reduced decreasing the sensitivity. Using the two-mode squeezing prediction for the variance and number of excitations the optimal scaled sensitivity is $27/(8N)$ showing Heisenberg limited scaling [69].

The inset of Fig. 4 shows the time evolution of the scaled sensitivity for a range of different system sizes, demonstrating superlinear sensitivity gains beyond the standard quantum

limit. In the main panel of Fig. 4 we analyze the scaling of the optimal sensitivity with system size for both the staggered z field (open symbols) and the Floquet-engineered model (filled symbols) for different power-law exponents α . Notably, for large layer spacings all power-law exponents collapse onto the same scaling. However, we observe two distinct scaling behaviors: the staggered field model shows $1/\sqrt{N}$ scaling, whereas the Floquet-engineered model achieves the optimal Heisenberg limit of $1/N$ scaling. Thus using Floquet-engineered interactions provides a significant improvement in sensitivity for all system sizes and achieves the best possible scaling.

Outlook. Our work demonstrates the scalable and robust generation of entanglement in the form of two-mode squeezed states separated in bilayers of power-law interacting quantum spin models.

This extends the feasibility of two-mode squeezing to generic power-law models, making it accessible in a significantly larger number of experimental platforms. In particular, we show that finite-range interactions ($\alpha = 1, 2, 3$) can achieve the same amount of entanglement and squeezing as infinite-range interactions ($\alpha = 0$).

We further develop a Floquet protocol utilizing spatiotemporal control to engineer the spin-spin interactions. This has a number of immediate benefits. It extends the applicability of our results to models with Ising interactions in systems, which may not naturally realize Heisenberg interactions. In addition, the Floquet-engineered model achieves the optimal Heisenberg scaling of the sensitivity, providing potentially orders of magnitude improvements. Finally, it also allows one to implement time reversal by reversing the interlayer spin-exchange interactions, which may be used for time-reversal based metrological protocols.

This establishes spatiotemporally engineered interactions adapted to the initial state and the desired dynamics as a viable pathway to unlocking significant quantum advantage beyond that present in naturally occurring interactions. It highlights the great potential in making full use of the control inherent in state-of-the-art current experimental platforms realizing fully controllable quantum spin systems for entanglement generation and quantum sensing.

Acknowledgments. The calculations were performed in the PETE system of the High Performance Computing Center at Oklahoma State University, NSF Grant No. OAC-1531128.

- [1] M. A. Baranov, M. Dalmonte, G. Pupillo, and P. Zoller, Condensed matter theory of dipolar quantum gases, *Chem. Rev.* **112**, 5012 (2012).
- [2] J. L. Bohn, A. M. Rey, and J. Ye, Cold molecules: Progress in quantum engineering of chemistry and quantum matter, *Science* **357**, 1002 (2017).
- [3] S. A. Moses, J. P. Covey, M. T. Miecniowski, D. S. Jin, and J. Ye, New frontiers for quantum gases of polar molecules, *Nat. Phys.* **13**, 13 (2017).
- [4] L. Chomaz, I. Ferrier-Barbut, F. Ferlaino, B. Laburthe-Tolra, B. L. Lev, and T. Pfau, Dipolar physics: A review of experiments with magnetic quantum gases, *Rep. Prog. Phys.* **86**, 026401 (2023).
- [5] A. Browaeys and T. Lahaye, Many-body physics with individually controlled Rydberg atoms, *Nat. Phys.* **16**, 132 (2020).
- [6] M. Saffman, T. G. Walker, and K. Mølmer, Quantum information with Rydberg atoms, *Rev. Mod. Phys.* **82**, 2313 (2010).
- [7] C. Monroe, W. C. Campbell, L.-M. Duan, Z.-X. Gong, A. V. Gorshkov, P. W. Hess, R. Islam, K. Kim, N. M. Linke, G. Pagano, P. Richerme, C. Senko, and N. Y. Yao, Programmable quantum simulations of spin systems with trapped ions, *Rev. Mod. Phys.* **93**, 025001 (2021).
- [8] I. Bloch, J. Dalibard, and S. Nascimbène, Quantum simulations with ultracold quantum gases, *Nat. Phys.* **8**, 267 (2012).
- [9] C. Gross and I. Bloch, Quantum simulations with ultracold atoms in optical lattices, *Science* **357**, 995 (2017).

- [10] A. J. Daley, I. Bloch, C. Kokail, S. Flannigan, N. Pearson, M. Troyer, and P. Zoller, Practical quantum advantage in quantum simulation, *Nature (London)* **607**, 667 (2022).
- [11] H.-J. Briegel, T. Calarco, D. Jaksch, J. I. Cirac, and P. Zoller, Quantum computing with neutral atoms, *J. Mod. Opt.* **47**, 415 (2000).
- [12] M. Morgado and S. Whitlock, Quantum simulation and computing with Rydberg-interacting qubits, *AVS Quantum Sci.* **3**, 023501 (2021).
- [13] L. Henriët, L. Beguin, A. Signoles, T. Lahaye, A. Browaeys, G.-O. Reymond, and C. Jurczak, Quantum computing with neutral atoms, *Quantum* **4**, 327 (2020).
- [14] L. Pezzè, A. Smerzi, M. K. Oberthaler, R. Schmied, and P. Treutlein, Quantum metrology with nonclassical states of atomic ensembles, *Rev. Mod. Phys.* **90**, 035005 (2018).
- [15] A. M. Kaufman and K.-K. Ni, Quantum science with optical tweezer arrays of ultracold atoms and molecules, *Nat. Phys.* **17**, 1324 (2021).
- [16] C. Gross and W. S. Bakr, Quantum gas microscopy for single atom and spin detection, *Nat. Phys.* **17**, 1316 (2021).
- [17] L. Anderegg, L. W. Cheuk, Y. Bao, S. Burchesky, W. Ketterle, K.-K. Ni, and J. M. Doyle, An optical tweezer array of ultracold molecules, *Science* **365**, 1156 (2019).
- [18] L. Christakis, J. S. Rosenberg, R. Raj, S. Chi, A. Morningstar, D. A. Huse, Z. Z. Yan, and W. S. Bakr, Probing site-resolved correlations in a spin system of ultracold molecules, *Nature (London)* **614**, 64 (2023).
- [19] C. M. Holland, Y. Lu, and L. W. Cheuk, On-demand entanglement of molecules in a reconfigurable optical tweezer array, *Science* **382**, 1143 (2023).
- [20] Y. Bao, S. S. Yu, L. Anderegg, E. Chae, W. Ketterle, K.-K. Ni, and J. M. Doyle, Dipolar spin-exchange and entanglement between molecules in an optical tweezer array, *Science* **382**, 1138 (2023).
- [21] T. Oka and S. Kitamura, Floquet engineering of quantum materials, *Annu. Rev. Condens. Matter Phys.* **10**, 387 (2019).
- [22] C. Weitenberg and J. Simonet, Tailoring quantum gases by floquet engineering, *Nat. Phys.* **17**, 1342 (2021).
- [23] J. Choi, H. Zhou, H. S. Knowles, R. Landig, S. Choi, and M. D. Lukin, Robust dynamic hamiltonian engineering of many-body spin systems, *Phys. Rev. X* **10**, 031002 (2020).
- [24] H. Zhou, L. S. Martin, M. Tyler, O. Makarova, N. Leitao, H. Park, and M. D. Lukin, Robust higher-order hamiltonian engineering for quantum sensing with strongly interacting systems, *Phys. Rev. Lett.* **131**, 220803 (2023).
- [25] A. Periwal, E. S. Cooper, P. Kunkel, J. F. Wienand, E. J. Davis, and M. Schleier-Smith, Programmable interactions and emergent geometry in an array of atom clouds, *Nature (London)* **600**, 630 (2021).
- [26] N. Nishad, A. Keselman, T. Lahaye, A. Browaeys, and S. Tsesses, Quantum simulation of generic spin-exchange models in floquet-engineered Rydberg-atom arrays, *Phys. Rev. A* **108**, 053318 (2023).
- [27] P. Scholl, H. J. Williams, G. Bornet, F. Wallner, D. Barredo, L. Henriët, A. Signoles, C. Hainaut, T. Franz, S. Geier, A. Tebben, A. Salzinger, G. Zürn, T. Lahaye, M. Weidemüller, and A. Browaeys, Microwave engineering of programmable XXZ hamiltonians in arrays of Rydberg atoms, *PRX Quantum* **3**, 020303 (2022).
- [28] S. Geier, N. Thaicharoen, C. Hainaut, T. Franz, A. Salzinger, A. Tebben, D. Grimshandl, G. Zürn, and M. Weidemüller, Floquet hamiltonian engineering of an isolated many-body spin system, *Science* **374**, 1149 (2021).
- [29] C. Miller, A. N. Carroll, J. Lin, H. Hirzler, H. Gao, H. Zhou, M. D. Lukin, and J. Ye, Two-axis twisting using floquet-engineered XYZ spin models with polar molecules, *arXiv:2404.18913*.
- [30] W. Morong, K. S. Collins, A. De, E. Stavropoulos, T. You, and C. Monroe, Engineering dynamically decoupled quantum simulations with trapped ions, *PRX Quantum* **4**, 010334 (2023).
- [31] D. J. Wineland, J. J. Bollinger, W. M. Itano, F. L. Moore, and D. J. Heinzen, Spin squeezing and reduced quantum noise in spectroscopy, *Phys. Rev. A* **46**, R6797 (1992).
- [32] D. J. Wineland, J. J. Bollinger, W. M. Itano, and D. J. Heinzen, Squeezed atomic states and projection noise in spectroscopy, *Phys. Rev. A* **50**, 67 (1994).
- [33] G. Vasilakis, H. Shen, K. Jensen, M. Balabas, D. Salart, B. Chen, and E. S. Polzik, Generation of a squeezed state of an oscillator by stroboscopic back-action-evading measurement, *Nat. Phys.* **11**, 389 (2015).
- [34] J. Appel, P. J. Windpassinger, D. Oblak, U. B. Hoff, N. Kjærgaard, and E. S. Polzik, Mesoscopic atomic entanglement for precision measurements beyond the standard quantum limit, *Proc. Natl. Acad. Sci. USA* **106**, 10960 (2009).
- [35] M. H. Schleier-Smith, I. D. Leroux, and V. Vuletić, States of an ensemble of two-level atoms with reduced quantum uncertainty, *Phys. Rev. Lett.* **104**, 073604 (2010).
- [36] J. G. Bohnet, K. C. Cox, M. A. Norcia, J. M. Weiner, Z. Chen, and J. K. Thompson, Reduced spin measurement back-action for a phase sensitivity ten times beyond the standard quantum limit, *Nat. Photon.* **8**, 731 (2014).
- [37] R. J. Sewell, M. Koschorreck, M. Napolitano, B. Dubost, N. Behbood, and M. W. Mitchell, Magnetic sensitivity beyond the projection noise limit by spin squeezing, *Phys. Rev. Lett.* **109**, 253605 (2012).
- [38] H. Bao, J. Duan, S. Jin, X. Lu, P. Li, W. Qu, M. Wang, I. Novikova, E. E. Mikhailov, K.-F. Zhao *et al.*, Spin squeezing of 1011 atoms by prediction and retrodiction measurements, *Nature (London)* **581**, 159 (2020).
- [39] W. J. Eckner, N. Darkwah Oppong, A. Cao, A. W. Young, W. R. Milner, J. M. Robinson, J. Ye, and A. M. Kaufman, Realizing spin squeezing with Rydberg interactions in an optical clock, *Nature (London)* **621**, 734 (2023).
- [40] J. Franke, S. R. Muleady, R. Kaubruegger, F. Kranzl, R. Blatt, A. M. Rey, M. K. Joshi, and C. F. Roos, Quantum-enhanced sensing on optical transitions through finite-range interactions, *Nature (London)* **621**, 740 (2023).
- [41] G. Bornet, G. Emperauger, C. Chen, B. Ye, M. Block, M. Bintz, J. A. Boyd, D. Barredo, T. Comparin, F. Mezzacapo, T. Roscilde, T. Lahaye, N. Y. Yao, and A. Browaeys, Scalable spin squeezing in a dipolar Rydberg atom array, *Nature (London)* **621**, 728 (2023).
- [42] J. A. Hines, S. V. Rajagopal, G. L. Moreau, M. D. Wahrman, N. A. Lewis, O. Marković, and M. Schleier-Smith, Spin squeezing by Rydberg dressing in an array of atomic ensembles, *Phys. Rev. Lett.* **131**, 063401 (2023).
- [43] G. Agarwal, *Quantum Optics* (Cambridge University Press, Cambridge, UK, 2013).

- [44] C. M. Caves and B. L. Schumaker, New formalism for two-photon quantum optics. I. Quadrature phases and squeezed states, *Phys. Rev. A* **31**, 3068 (1985).
- [45] B. L. Schumaker and C. M. Caves, New formalism for two-photon quantum optics. II. Mathematical foundation and compact notation, *Phys. Rev. A* **31**, 3093 (1985).
- [46] M. D. Reid, P. D. Drummond, W. P. Bowen, E. G. Cavalcanti, P. K. Lam, H. A. Bachor, U. L. Andersen, and G. Leuchs, Colloquium: The Einstein-Podolsky-Rosen paradox: From concepts to applications, *Rev. Mod. Phys.* **81**, 1727 (2009).
- [47] J. Hu, L. Feng, Z. Zhang, and C. Chin, Quantum simulation of unruh radiation, *Nat. Phys.* **15**, 785 (2019).
- [48] P. Hauke, D. Marcos, M. Dalmonte, and P. Zoller, Quantum simulation of a lattice schwinger model in a chain of trapped ions, *Phys. Rev. X* **3**, 041018 (2013).
- [49] V. Kasper, F. Hebenstreit, M. Oberthaler, and J. Berges, Schwinger pair production with ultracold atoms, *Phys. Lett. B* **760**, 742 (2016).
- [50] A. Heidmann, R. J. Horowicz, S. Reynaud, E. Giacobino, C. Fabre, and G. Camy, Observation of quantum noise reduction on twin laser beams, *Phys. Rev. Lett.* **59**, 2555 (1987).
- [51] B. Julsgaard, A. Kozhekin, and E. S. Polzik, Experimental long-lived entanglement of two macroscopic objects, *Nature (London)* **413**, 400 (2001).
- [52] N. J. Cerf, G. Leuchs, and E. S. Polzik, *Quantum Information with Continuous Variables of Atoms and Light* (World Scientific, Singapore, 2007).
- [53] C. Gross, H. Strobel, E. Nicklas, T. Zibold, N. Bar-Gill, G. Kurizki, and M. K. Oberthaler, Atomic homodyne detection of continuous-variable entangled twin-atom states, *Nature (London)* **480**, 219 (2011).
- [54] B. Lücke, M. Scherer, J. Kruse, L. Pezzé, F. Deuretzbacher, P. Hyllus, O. Topic, J. Peise, W. Ertmer, J. Arlt, L. Santos, A. Smerzi, and C. Klempt, Twin matter waves for interferometry beyond the classical limit, *Science* **334**, 773 (2011).
- [55] E. M. Bookjans, C. D. Hamley, and M. S. Chapman, Strong quantum spin correlations observed in atomic spin mixing, *Phys. Rev. Lett.* **107**, 210406 (2011).
- [56] A. T. Black, E. Gomez, L. D. Turner, S. Jung, and P. D. Lett, Spinor dynamics in an antiferromagnetic spin-1 condensate, *Phys. Rev. Lett.* **99**, 070403 (2007).
- [57] L. Zhao, J. Jiang, T. Tang, M. Webb, and Y. Liu, Dynamics in spinor condensates tuned by a microwave dressing field, *Phys. Rev. A* **89**, 023608 (2014).
- [58] A. Qu, B. Evrard, J. Dalibard, and F. Gerbier, Probing spin correlations in a Bose-Einstein condensate near the single-atom level, *Phys. Rev. Lett.* **125**, 033401 (2020).
- [59] K. Kim, J. Hur, S. J. Huh, S. Choi, and J.-Y. Choi, Emission of spin-correlated matter-wave jets from spinor Bose-Einstein condensates, *Phys. Rev. Lett.* **127**, 043401 (2021).
- [60] K. Lange, J. Peise, B. Lücke, I. Kruse, G. Vitagliano, I. Apellaniz, M. Kleinmann, G. Tóth, and C. Klempt, Entanglement between two spatially separated atomic modes, *Science* **360**, 416 (2018).
- [61] M. Fadel, T. Zibold, B. Décamps, and P. Treutlein, Spatial entanglement patterns and Einstein-Podolsky-Rosen steering in Bose-Einstein condensates, *Science* **360**, 409 (2018).
- [62] P. Kunkel, M. Prüfer, H. Strobel, D. Linnemann, A. Frölian, T. Gasenzer, M. Gärtner, and M. K. Oberthaler, Spatially distributed multipartite entanglement enables EPR steering of atomic clouds, *Science* **360**, 413 (2018).
- [63] B. Sundar, D. Barberena, A. P. Orioli, A. Chu, J. K. Thompson, A. M. Rey, and R. J. Lewis-Swan, Bosonic pair production and squeezing for optical phase measurements in long-lived dipoles coupled to a cavity, *Phys. Rev. Lett.* **130**, 113202 (2023).
- [64] T. Bilitewski and A. M. Rey, Manipulating growth and propagation of correlations in dipolar multilayers: From pair production to bosonic Kitaev models, *Phys. Rev. Lett.* **131**, 053001 (2023).
- [65] T. Bilitewski, G. A. Domínguez-Castro, D. Wellnitz, A. M. Rey, and L. Santos, Tunable momentum pair creation of spin excitations in dipolar bilayers, *Phys. Rev. A* **108**, 013313 (2023).
- [66] W. G. Tobias, K. Matsuda, J.-R. Li, C. Miller, A. N. Carroll, T. Bilitewski, A. M. Rey, and J. Ye, Reactions between layer-resolved molecules mediated by dipolar spin exchange, *Science* **375**, 1299 (2022).
- [67] S. Hawaldar, P. Shahi, A. L. Carter, A. M. Rey, J. J. Bollinger, and A. Shankar, Bilayer crystals of trapped ions for quantum information processing, [arXiv:2312.10681](https://arxiv.org/abs/2312.10681).
- [68] Z. Meng, L. Wang, W. Han, F. Liu, K. Wen, C. Gao, P. Wang, C. Chin, and J. Zhang, Atomic Bose-Einstein condensate in twisted-bilayer optical lattices, *Nature (London)* **615**, 231 (2023).
- [69] See Supplemental Material at <http://link.aps.org/supplemental/10.1103/PhysRevA.109.L061304> for additional details on the comparison of the dTWA simulations to exact numerics for finite and infinite-range ($\alpha = 0$) interactions, convergence of the Floquet dynamics to the dynamics under the effective Hamiltonian, extended results on the behavior of the collective layer spins for all interaction ranges, a comparison of the two-mode squeezing predictions with the spin dynamics for squeezed and antisqueezed quadratures and for the sensitivity, and the dynamics for finite lattice filling fractions.
- [70] T. Holstein and H. Primakoff, Field dependence of the intrinsic domain magnetization of a ferromagnet, *Phys. Rev.* **58**, 1098 (1940).
- [71] J. Schachenmayer, A. Pikovski, and A. M. Rey, Many-body quantum spin dynamics with Monte Carlo trajectories on a discrete phase space, *Phys. Rev. X* **5**, 011022 (2015).
- [72] B. Zhu, A. M. Rey, and J. Schachenmayer, A generalized phase space approach for solving quantum spin dynamics, *New J. Phys.* **21**, 082001 (2019).
- [73] S. R. Muleady, M. Yang, S. R. White, and A. M. Rey, Validating phase-space methods with tensor networks in two-dimensional spin models with power-law interactions, *Phys. Rev. Lett.* **131**, 150401 (2023).